Hindawi
Advances in Civil Engineering
Volume 2021, Article ID 8847771, 15 pages
https://doi.org/10.1155/2021/8847771

Research Article

Modal Analysis of Beam Structures with Random Field Models at Multiple Scales

Dan Feng [1,2]

[1]*Economics and Management School of Wuhan University, Wuhan 420106, China*
[2]*China Construction Seventh Engineering Division. Corp. Ltd, Zhengzhou 450004, China*

Correspondence should be addressed to Dan Feng; 2017101050083@whu.edu.cn

Received 10 July 2020; Revised 13 August 2020; Accepted 18 December 2020; Published 4 January 2021

Academic Editor: Yi Zhang

Structure material properties are heterogeneous in nature and would be characterized with different statistics at different length scales due to the spatially averaging effects. This work develops a framework for the modal analysis of beam structures with random field models at multiple scales. In this framework, the random field theory is adopted to model heterogeneous material properties, and the cross-correlations between material properties are explicitly considered. The modal parameters of a structure are then evaluated using the finite element (FE) method with the simulated heterogeneous material properties taken as input. With the aid of Monte Carlo simulation, the modal parameters are analyzed in a probabilistic manner. In addition, to accommodate the necessity of different mesh sizes in FE models, an approach of evaluating random field parameters and generating random field material properties at different length scales is developed. The performance of the proposed framework is demonstrated through the modal analysis of a simply supported beam, where the formulation of the multiscale random field approach is validated and the effects of heterogeneous material properties on modal parameters are analyzed. Parametric studies on the random field parameters, including the coefficient of variation and the scale of fluctuation, are also conducted to further investigate the relations between the random field parameters at different scales.

1. Introduction

To evaluate the sustainability of structures (e.g., buildings and bridges) is a long-lasting problem in civil engineering community [1–3]. Structures are often subjected to dynamic loads, such as winds, waves, earthquakes, traffic, and human activities, which could gradually deteriorate the life-long sustainability of a structure. The force magnitudes or directions of dynamic loads keep varying with time, leading structures to exhibit complex mechanical behaviours. Modal parameters, including modal frequencies, mode shapes, modal masses, and modal damping ratios, are a set of inherent parameters that characterize the dynamic properties of a structure [4]. Despite the changeable nature of dynamic loads, modal parameters keep constant and are independent of the types and ranges of the external dynamic loads [5]. Modal analysis aims at determining the modal parameters of a structure and hence has become an essential task for a wide range of applications, such as serviceability analysis [6], vibration control [7, 8], load estimation [9], structural damage identification [10, 11], and structural health monitoring [12, 13].

The theories and methods to determine the modal parameters of a structure are relatively well developed. For structures with simple geometries, e.g., cantilever beam, plate, or shell structures, the analytical solutions of their modal parameters might be available [4]. In regard to complex structures with arbitrary shapes and various constituents, the finite element (FE) method is usually employed to approximate the modal parameters in a discrete manner [14–17]. Technically, the modal parameters of a structure are determined completely by its material properties (e.g., mass, stiffness, damping, etc.) [4]. In earlier years, studies on modal analysis considered structures such as homogeneous materials for simplicity (e.g., [14, 15]). However, the material properties of a structure are spatially variable in nature [18–24]. The spatial variability could result from various factors, such as fluctuations in material constituents, fracture

defects, and variable historic loading conditions. Recently, modal analysis with the consideration of spatially varying material parameters has been on the rise [25–28], partially due to the development of probabilistic FE analysis strategies and the increase in computational power.

Within the studies of probabilistic modal analysis, the approaches of simulating a heterogeneous structure can be basically classified into two categories: the random variable approach and the random field approach. In the random variable approach, the material properties of a structure are modelled as a set of random variables that are independent with each other (i.e., without any correlation). This approach is most suitable for modelling structures that consist of simple components, and each component is discretized into a single element during the FE analysis. For example, Ding et al. [29] introduced a 1% uncertainty with Gaussian distributions into the elemental stiffness parameters of a planar truss structure to account for the modelling errors. In the random field approach, the material property is modelled by a set of random variables with an autocorrelation. That is, two elements in the vicinity of each other tend to have similar material properties due to a high correlation with each other. Such correlation decreases with the increasing separation distance between those two elements. The second category, i.e., the random field approach, is more appropriate for modelling continuous structures. In this category, for example, Su et al. [26] considered Young's modulus and density of a simply supported beam as a random field with a normal distribution and developed a reliability-based method for structural damage identification based on the response surface method and Monte Carlo simulation (MCS).

In reference to the random field approach, a random field is generally characterized by two components: a distribution model that describes the probability density distribution of all the possible values of a material property at different locations and a correlation function that describes the correlation between the material properties of two locations. There are classical solutions for the distribution model (e.g., normal distribution and lognormal distribution [30]) and correlation function (e.g., single exponential function [31]), the parameters of which are usually determined through a site investigation process [32–34]. Currently, the random field theory has been widely used in geotechnical engineering to address the random heterogeneity of natural and artificial soils [35–39]. It has led to many inspiring studies in a wide range of applications. For example, the random field theory has been used to perform probabilistic stability analyses of slopes and footings [40, 41], to perform probabilistic evaluation of seabed liquefaction [42, 43], to depict the effectiveness of soil compaction [44], and to characterize the levels of soil contamination [45]. The application of the random field theory in structural engineering for characterizing structure material properties is comparably less, whereas it is on the rise recently.

When applying the random field approach to simulate a heterogeneous structure, it is important to recognize that the statistics of a material property are determined upon elements with a specific size, i.e., the size of testing samples during site investigation. There could be considerable discrepancies between the statistics of elements with different sizes. For example, the variance of a material property of a large element tends to be smaller than that of a smaller element due to the spatially averaging effects. Thus, the random field parameters characterized at a certain scale cannot be directly applied to generate a random field of material property at another scale. However, in FE analysis, the mesh size does not need to be the same as the size of the testing samples. There are cases in which large element sizes are adopted to reduce computational expenses. Modelling a heterogeneous material at different scales, which is essential in the FE-based structural modal analysis, remains a topic less explored. Key knowledge gaps exist in generating random field material properties at different scales and in understanding the scale effects on modal analysis.

This work aims to develop a framework for the probabilistic characterization of structural dynamics with random field models at multiple scales. In particular, an approach of evaluating random field parameters and generating random field material properties at different scales is developed to accommodate the necessity of different mesh sizes in the FE-based structural modal analysis. The remainder of this paper is organized as follows. Section 2 details the formulation of the random field models at multiple scales. Section 3 describes the framework of the probabilistic FE-based structural modal analysis. Section 4 reports the results of an illustrative example using a simply supported beam, through which the formulation of the multiscale random field model is validated and the scale effects on the modal parameters of a structure are investigated. Based upon the results presented, concluding remarks of this work are summarized in Section 5.

2. Multiscale Random Field Models

2.1. Simulation of a Random Field. It is known that material properties of a structure vary in space with an autocorrelation structure. The random field theory is an effective method for simulating such spatially varying and autocorrelated material properties [46–50]. For simplicity, this work focuses on stationary random fields, where (1) the distribution, as well as the corresponding statistics, of each variable remains constant everywhere and (2) the correlation between the variables at different locations depends only on the separation distance [51, 52]. A nonstationary field can be transformed into a stationary field by removing a lower-order polynomial trend [51] or by applying a space deformation [53].

Mathematically, a random field can be quantified as a set of random variables at various locations, and these variables are compliant to a joint multivariate distribution [20, 39]. Considering a stationary Gaussian field with a number of n locations of interest, the random field can be quantified as a set of random variables $\mathbf{Z}$, with $\mathbf{Z} = [Z_1, Z_2, \ldots, Z_n]$ representing the material property value at locations $i = 1, 2, \ldots, n$. The correlation between variables Z_i and Z_j can be described by a correlation function $\rho(\Delta x)$, where the underlying variable Δx represents the separation distance

between locations i and j. For example, a single exponential function [31], as adopted in this work, is written as

$$\rho(\Delta x) = \exp\left(-\frac{2\Delta x}{\theta}\right), \tag{1}$$

where θ is the scale of fluctuation. The Cholesky decomposition approach developed by [54] is an effective method to generate realizations of random but autocorrelated variables. By using Cholesky decomposition, the correlated random variables can be related to a set of independent random variables through

$$\mathbf{Z} = \mathbf{LU}, \tag{2}$$

where $\mathbf{U}$ is a vector of independent random variables with the same statistics of variable $\mathbf{Z}$ and $\mathbf{L}$ is the Cholesky decomposition of covariance matrix $\mathbf{C}$ satisfying $\mathbf{C} = \mathbf{LL}^T$. The covariance matrix $\mathbf{C}$ consists of components ρ_{ij} (calculated from equation (1)), which characterize the covariance of the material property values at location $\mathbf{x}_i$ and $\mathbf{x}_j$.

Insomuch that there are multiple material properties and these material properties exhibit a cross-correlation between each other, these multiple material properties can be simulated following a similar Cholesky decomposition process [49, 55, 56].

$$\mathbf{X}^{[n\times m]} = \mathbf{Z}^{[n\times m]}\left(\mathbf{L}'^{[m\times m]}\right)^T, \tag{3}$$

where $\mathbf{X}^{[n\times m]}$ represents the matrix of m cross-correlated material properties at n locations, $\mathbf{Z}^{[n\times m]}$ represents the value matrix of the m cross-independent material properties at n locations simulated from equation (2), and $\mathbf{L}'^{[m\times m]}$ represents the Cholesky decomposition of the covariance matrix $\mathbf{R}$, of which the component R_{ij} represents the covariance between the material properties $\mathbf{X}_i$ and $\mathbf{X}_j$, where $i, j = 1, 2, \ldots, m$ are the material property indexes.

2.2. Random Field Parameters at Different Scales. As mentioned above, the statistics of a random field are evaluated from testing samples with a certain size. In order to establish a relation between the random field parameters at different scales, it is assumed that the value of a material property at the coarse scale is an average of the values of this material property at the corresponding fine-scale locations. As an example shown in Figure 1, an element at the coarse scale corresponds to four elements at the fine scale. The value of material property Z^c at the coarse scale is approximated by averaging the four values Z_i^f at the fine scale. Generally, the relation between material property values at different scales, by averaging effects, can be given as [20]

$$Z^c = \frac{1}{N}\sum_i^N Z_i^f, \tag{4}$$

where N is the number of fine-scale elements that covers by a coarse-scale element.

Assuming that the random field parameters (e.g., mean, standard deviation, and correlation) of a material property are given at the fine scale, the statistics of this material property at the coarse scale can be derived through equation (4). Specifically, the mean of Z^c can be obtained by taking the expectation of equation (4), such that

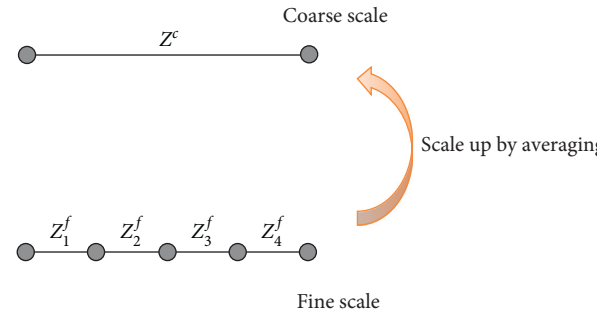

Figure 1: Illustration of the material properties at coarse and fine scales and the averaging effect.

$$\mu_{Z^c} = E\left(\frac{1}{N}\sum_i^N Z_i^f\right) = \frac{1}{N}\sum_i^N Z_i^f, \tag{5}$$

where $E(\cdot)$ represents the expectation operator. Accordingly, the variance is calculated as

$$\sigma_{Z^c}^2 = E\left((Z^c)^2\right) - E(Z^c)^2 = \frac{1}{N^2}\sum_i^N\sum_j^N \rho_{Z_i^f Z_j^f}\sigma_{Z_i^f}\sigma_{Z_j^f} - \mu_{Z^c}^2, \tag{6}$$

where $\rho_{Z_i^f Z_j^f}$ represents the correlation between material properties at locations i and j at the fine scale. By definition, the correlation between material properties at locations i and j at the coarse scale is given as

$$\rho_{Z_i^c Z_j^c} = \frac{\mathrm{COV}\left(Z_i^c, Z_j^c\right)}{\sigma_{Z_i^c}\sigma_{Z_j^c}} = \frac{E\left(Z_i^c Z_j^c\right) - E\left(Z_i^c\right)E\left(Z_j^c\right)}{\sigma_{Z_i^c}\sigma_{Z_j^c}}, \tag{7}$$

where $\mathrm{COV}(\cdot)$ represents the variance operator. In a similar fashion, substituting Z_i^c and Z_j^c with equation (4) and simplifying yields

$$\rho_{Z_i^c Z_j^c} = \frac{\left(\left(1/N^2\right)\sum_k^N\sum_l^N \rho_{Z_{i,k}^f Z_{j,l}^f}\sigma_{Z_{i,k}^f}\sigma_{Z_{j,l}^f} - \mu_{Z_i^c}\mu_{Z_j^c}\right)}{\sigma_{Z_i^c}\sigma_{Z_j^c}}, \tag{8}$$

where variables $Z_{i,k}$ and $Z_{j,l}$ represent the values of material property at fine-scale elements k and l that correspond to coarse-scale elements i and j, respectively.

With the random field statistics given at the fine scale, the random field statistics at the coarse scale can be evaluated based on the formulations presented above. By virtue of the theorem that a linear combination of a multivariate normal random vector also has a normal distribution [30], the material property at the coarse scale, as an average of the material property values at the fine scale, also exhibits a Gaussian random field. Random fields of material properties at the coarse scale can then be simulated following the general procedures provided in Section 2.1.

2.3. Non-Gaussian Distributions. It is assumed in the previous section that the random field being considered is a Gaussian process. Besides normal distributions, the beta, gamma, and lognormal distributions are also commonly used and have their unique applications in natural and social sciences [20, 30]. In regard to the case that the fine-scale material properties follow a general distribution, the random field parameters at the coarse scale can still be evaluated using the same formulations presented in the previous section. However, the distribution of the coarse-scale material properties becomes an unknown. To resolve this problem, Chen et al. [20] proposed several options to approximate the coarse-scale distributions, which are summarized as follows.

(i) Empirical function: realizations of material properties at the fine scale are first simulated and averaged. Empirical probability density function or cumulative density function for the coarse-scale material property can then be obtained by fitting these simulated realizations.

(ii) Fine-scale distribution: when the number of fine-scale elements covered by a coarse-scale element is small, it is appropriate to approximate the coarse-scale material property using the same fine-scale distribution model, but with a different set of model parameters to reflect the statistics change after upscaling from fine scale to coarse scale (see equations (5) and (6)).

(iii) Gaussian distribution: when the number of fine-scale elements covered by a coarse-scale element is sufficiently large, in reference to the central limit theorem, it is more appropriate to approximate the coarse-scale material property using Gaussian distribution.

3. Framework of Probabilistic FE Analysis

The framework of probabilistic FE analysis of structural dynamics consists of three main components: (1) heterogeneous structural material properties are simulated using the random field theory; (2) with the simulated heterogeneous material properties, the modal parameters of a structure are evaluated based on FE models; and (3), with the aid of MCS, the modal parameters of this structure are analyzed in a probabilistic manner. This section presents the formulation of the FE-based modal analysis and the approach of integrating random fields into FE models.

3.1. FE-Based Modal Analysis. In reference to a general solid mechanics problem, the generalized equation of motion is given as

$$\nabla \cdot \boldsymbol{\sigma} + \rho \mathbf{b} = \rho \mathbf{a}, \tag{9}$$

where σ is the stress tensor, $\mathbf{b}$ is the body fore vector, $\mathbf{a}$ is the acceleration vector, and ρ is the material density. For the most basic problem involving a linear elastic material which obeys Hooke's Law, the matrix equations take the form of a dynamic spring mass system.

$$\mathbf{M}\ddot{U} + \mathbf{C}\dot{U} + \mathbf{K}\mathbf{U} = F, \tag{10}$$

where $\mathbf{M}$, $\mathbf{C}$, and $\mathbf{K}$ are the mass, damping, and stiffness matrices, respectively; $\mathbf{U}$ is the displacement vector; $[\ddot{\cdot}]$ and $[\dot{\cdot}]$ represent the first-order and second-order time derivative operators, respectively; and $\mathbf{F}$ is the force vector. For vibrational modal analysis, the damping is generally ignored, leaving only the first and third terms on the left-hand side [4]:

$$\mathbf{M}\ddot{U} + \mathbf{K}\mathbf{U} = 0, \tag{11}$$

which is the general form of the eigensystem encountered in structural engineering using FE analysis. The modal frequencies and mode shapes can be obtained by solving the generalized eigenvalue problem

$$\mathbf{K}\boldsymbol{\Phi} = \omega^2 \mathbf{M}\boldsymbol{\Phi}, \tag{12}$$

where ω and Φ represent the modal frequencies and mode shapes, respectively.

3.2. Integration with Random Field Material Properties. In FE analysis, the domain is discretized into a mesh, where the underlying material properties are also represented in a discrete manner. There are several strategies that can be employed to approximate material properties using their values at finite nodes, such as the midpoint method, the shape function method, the integration point method, the optimal linear estimation method, the spatial average method, and the weighted integral method [57]. In this work, the midpoint method, which was first introduced by Der Kiureghian and Ke [58], is adopted owing to its simplicity in implementation and computational efficiency. That is, the material property at each element is a constant and takes the material property value at the centroid of that element. To incorporate multiscale random fields in FE analysis, the target mesh size in a FE simulation is first determined, and the statistics of a material property at this target mesh size are calculated from the statistics of this material property at the reference scale using the multiscale random field approach. Then, the simulation domain is discretized into a mesh of the target mesh size and the material properties in each element are generated using the random field theory. Lastly, the random fields of material properties are imported into the FE simulation code so that each element has its specific material property value. With the incorporation of random fields, probabilistic FE analysis can be performed following the MCS scheme. The interested reader is also referred to [59, 60] for a general workflow of incorporating random fields in FE analysis. It should be noted that the MCS technique could be computationally expensive as it requires to run the simulation repeatedly for a large number of trials. There are several other approaches that are developed to improve computational efficiency, such as the subset simulation technique [61],

support vector machine method [62], and the Bayesian regression technique [63].

4. Numerical Simulations

In this section, a simply supported beam is taken as an example to verify the formulation of multiscale random field models and to investigate the effects of random field properties on the modal parameters of a structure. The beam has a span of 60 m (see Figure 2) with the cross-sectional area and the moment of inertia taken to be 11.2 m^2 and 20.87 m^4, respectively. In practice, the statistics of a material property at a reference scale could usually be determined through a site investigation process. Particularly, to determine the scales of fluctuation, the semi-variogram is first calculated and scales of fluctuation are determined by fitting the semi-variogram with an adopted correlation function [22]. With the statistics of a material property characterized from the testing samples at the reference scale, the statistics of this material property at a coarse scale could be determined using the developed multiscale random field approach. In this work, the fields of the mass density and Young's modulus along the beam are both assumed to follow a stationary Gaussian process with a cross-correlation. The statistics of the mass density and Young's modulus fields at the reference scale (i.e., mesh size of 0.5 m) are listed in Table 1. The cross-correlation between mass density and Young's modulus is taken as 0.8. This beam example has been previously studied in Su et al. [26] to demonstrate a reliability-based framework for damage identification. However, the cross-correlation between mass density and Young's modulus and the scale effects on random field statistics were not considered in that work.

4.1. General Results of Probabilistic Modal Analysis. To begin with, the simulation of random fields at different scales and the scale effects on the random field statistics are investigated. With the procedures described in Section 2.1, random fields of mass density and Young's modulus can be simulated, and example realizations of them are given in Figure 3. In this example realization, the mass density and Young's modulus at each location are random but varying spatially in a somewhat smooth manner. A positive cross-correlation between the mass density and Young's modulus can be identified by observing the phenomenon that locations with a larger mass density also exhibit a greater Young's modulus and vice versa.

For a probabilistic FE analysis considering random field material properties, MCSs are usually required to approach a statistical characterization of the structural dynamic responses. In this regard, 10,000 realizations of the mass density and Young's modulus are generated and will later be cast into the FE model to conduct modal analysis. Herein, the results of the 10,000 simulated random fields are first analyzed to investigate the effectiveness of the random field approach and MCSs. The material properties at the middle of the beam are probed, and the results of the histogram, mean, and coefficient of variation (COV) of the 10,000 realizations are gathered in Figure 4. As can be observed from the histograms, the distributions of mass density and Young's modulus appear as a bell curve and can be well fitted by normal distributions. As the number of MCSs increases, the mean and COV asymptotically approach their specified values.

With the 10,000 realizations of material properties, modal parameters of this beam are calculated, respectively. Figure 5 presents the statistics (i.e., histogram, mean, and COV) of the first-order modal frequencies based on the 10,000 MCSs. The values of modal frequency also appear as a normal distribution with a mean of 13.45 and a standard deviation of 0.33. The COV is calculated to be about 0.025, which is considerably large if comparing with the COV of mass density and Young's modulus (i.e., 0.05 and 0.1, respectively). The results indicate that the material heterogeneity has a considerably significant impact on the structure dynamic responses. Similar to the evolution pattern of material properties, the mean and COV of modal frequencies also asymptotically approach constants after a sufficient number of MCSs.

As the beam is discretized into 120 elements with 240 degrees of freedom, the mode shapes are vectors of 240 components. For visualization purposes, components corresponding to the deflections of the beam are extracted and rearranged and normalized to a unit vector. Figure 6 shows the profile of the first-order mode shape along the beam. The 90% confidence interval (CI) of the mode shape at each location forms a very tiny band, indicating relatively small variations due to material heterogeneity. To gain more insights into the effects of material heterogeneity on mode shapes, the modal assurance criterion (MAC) [64] is further investigated. The MAC is a statistical indicator that is most sensitive to large differences and relatively insensitive to small differences in the mode shapes. This yields a good statistic indicator and a degree of consistency between mode shapes [64]. In this work, the MAC values for mode shapes between the heterogeneous case and the homogeneous case are calculated and used to study the heterogeneity effects. Figure 7 shows the results of the histogram, mean, and COV of the first-order mode shape. For all 10,000 MCSs, the MAC values reside within a narrow range that from about 0.999 to 1. The mean of these MAC values is almost one, and the COV is next to zero (e.g., about $1.5e-4$). The results further indicate that material heterogeneity exhibits a considerably small impact on mode shapes.

4.2. Validation of Multiscale Random Field Models. In this section, the effectiveness of the proposed multiscale random field models will be investigated. With the random field statistics given at the reference scale, i.e., 0.5 m, the random field statistics at coarse scales can be calculated based on the proposed multiscale random field approach. In this work, mesh sizes of 2, 3, 4, 5, 6, and 8 times of the reference size are considered. After 10,000 MCSs, the statistics of the material property values of each

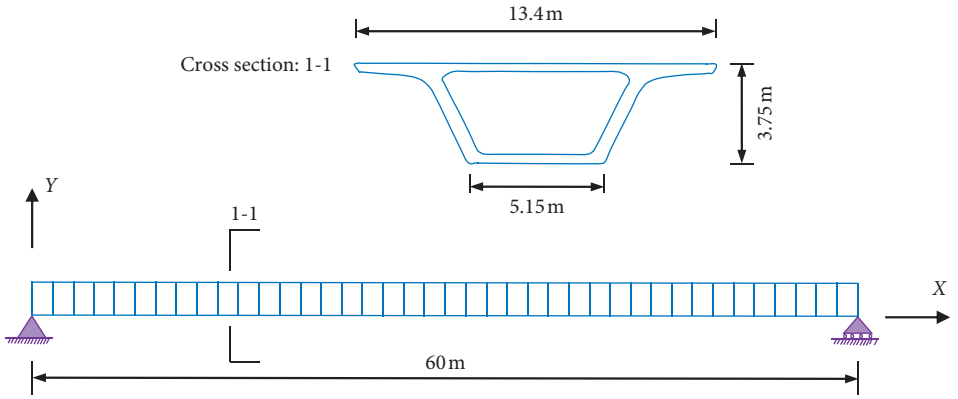

Figure 2: Geometry and boundary conditions of the example beam problem.

Table 1: Random field parameters of the mass density ρ and Young's modulus E of the example beam at the reference scale.

	Distribution	Mean	Coefficient of variation	Scale of fluctuation (m)
ρ	Normal	2500 kg/m3	0.05	30
E	Normal	32.5 GPa	0.10	30

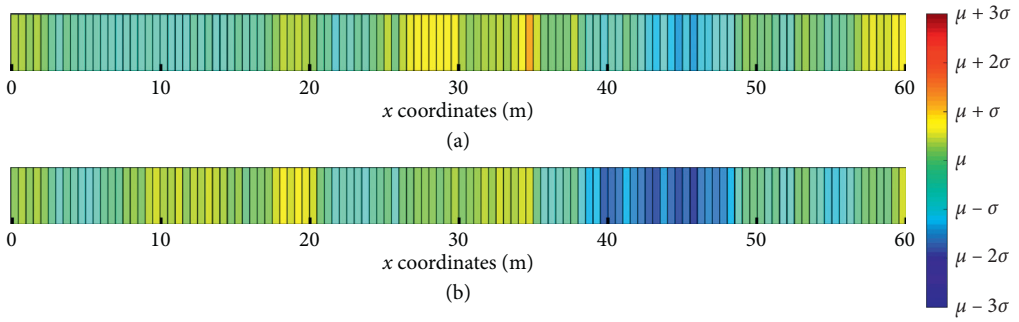

Figure 3: An example realization of the random fields of mass density and Young's modulus with 120 elements. The beam has a span of 60 m.

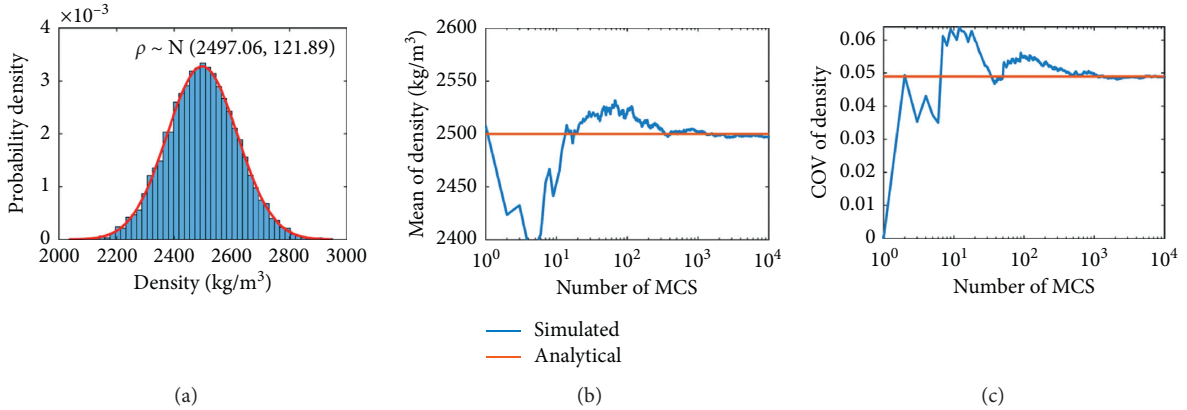

Figure 4: Continued.

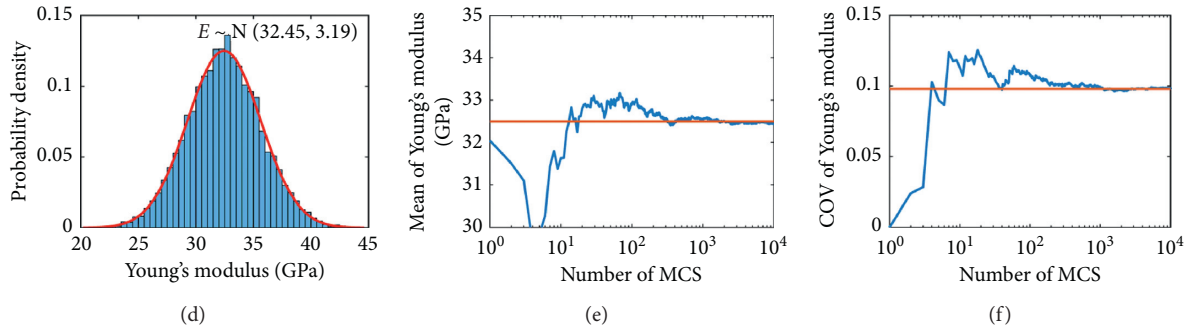

Figure 4: Histogram (a, d), mean (b, e), and COV (c, f) of the simulated random field properties within 10,000 MCSs. Top row and bottom row represent the results of mass density and Young's modulus, respectively.

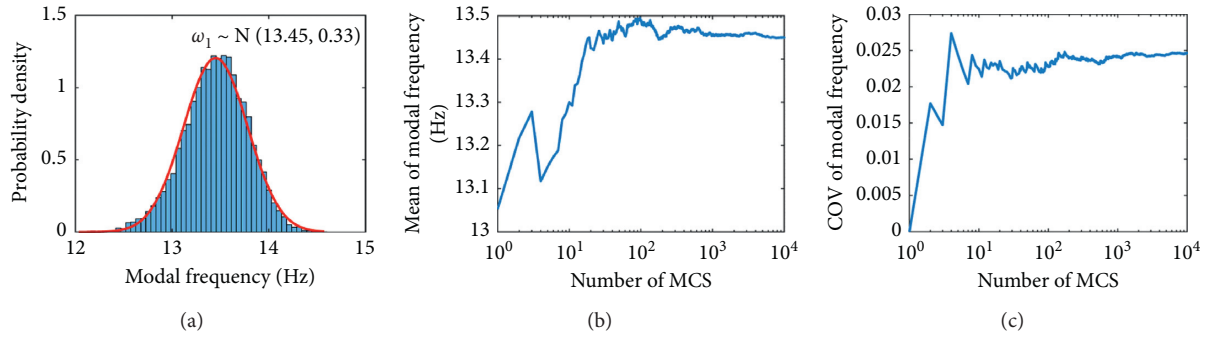

Figure 5: Histogram (a), mean (b), and COV (c) of the first-order modal frequencies based on 10,000 MCSs.

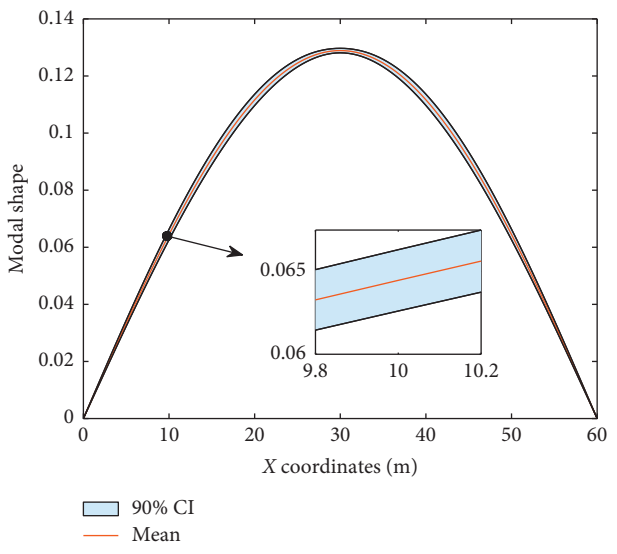

Figure 6: First-order mode shape with only the deflection components. The red line represents the mean of 10,000 MCSs, and the band represents 90% CI.

element are calculated and compared with the analytical solutions (i.e., equations (5), (6), and (8)). Figure 8 presents the COV of Young's modulus for the random fields at different scales. For each mesh, the COVs of each mesh element exhibit a slight variation, but all reside in a reasonable range around the analytical solution. The COV of Young's modulus decreases with the increasing mesh size, which is consistent with the fact of the spatially averaging effects.

The results of the correlation between material properties at different locations are presented in Figure 9. Basically, the correlation between material properties at two locations decreases with the increasing separation distances. With the same separation distances, the mesh elements with a greater size exhibit stronger correlation between each other than those with a smaller size. To better visualize the correlation change due to the mesh size effects, the magnitudes of correlation change of a coarse scale with respect to the reference scale are calculated, and both the analytical and simulated results are shown in Figure 9(b). Overall, the correlation changes based on analytic solution and simulated random fields exhibit very good agreement. The magnitudes of the correlation change due to the scale effects first increase with the increasing separation distances and then vanish as the correlation approaches zero.

Next, the effectiveness of using multiscale random fields for modal analysis is investigated. The modal analysis of the simply supported beam is conducted based on a mesh size of 4 m, i.e., 8 times that of the reference size 0.5 m. Random field material properties are generated using two approaches: (1) direct simulation, in which the random field material properties corresponding to the reference mesh size are first generated and are then added up and averaged to generate the random field material properties for the target mesh size; and (2) the proposed multiscale approach, in which the random field

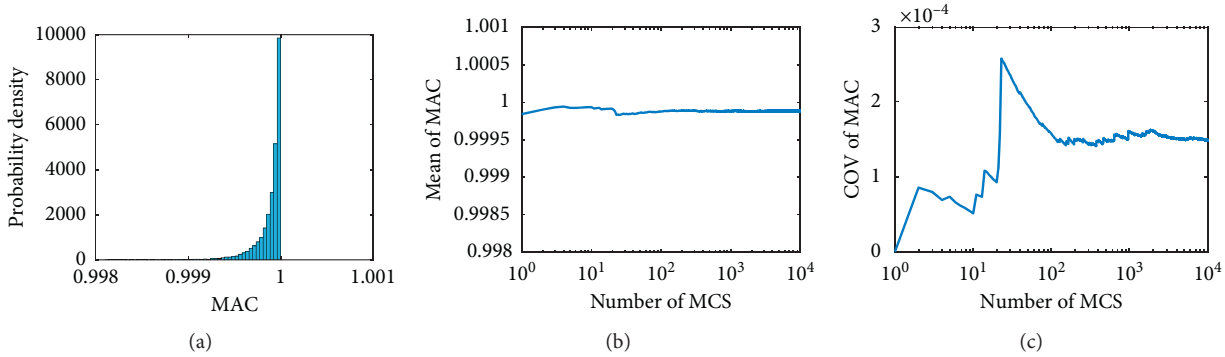

Figure 7: Histogram (a), mean (b), and COV (c) of the first-order MAC based on the 10,000 MCSs.

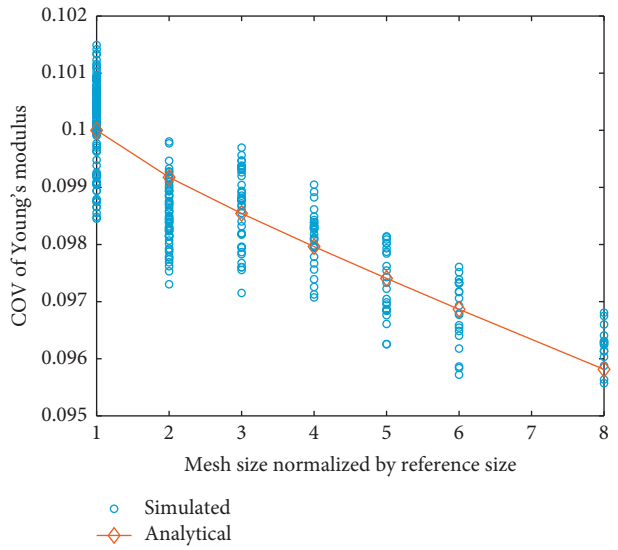

Figure 8: COV of Young's modulus for the random fields at different scales. Each point of the simulated data represents the COV of a mesh element based on the 10,000 MCSs.

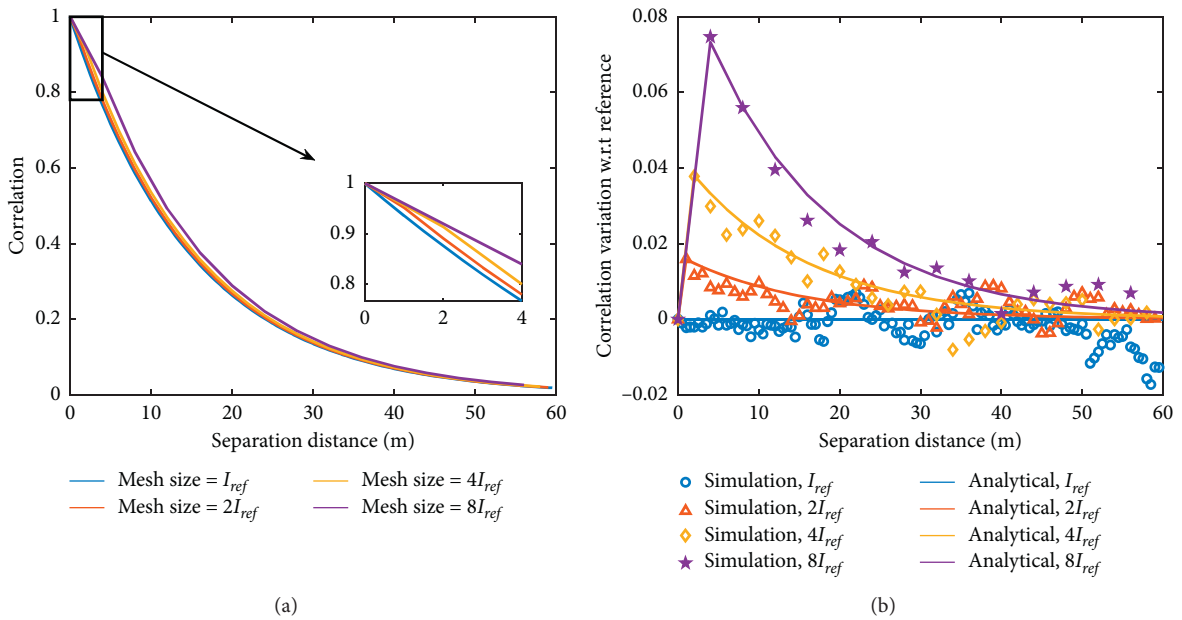

Figure 9: The correlation of material properties at different locations: (a) correlation vs. separation distance based on analytical formulations and (b) the change of correlation at a coarse scale with respect to the correlation at the reference scale based on the analytical formulations and the simulated random fields.

statistics for the target mesh size are first evaluated based on equations (5), (6), and (8) and then cast into the general procedures of simulating random fields to generate the random field material properties at the target scale. Herein, the direct simulation approach is adopted as a benchmark to verify the proposed multiscale approach. Figure 10 presents the cumulative distribution of the first- and sixth-order modal frequencies based on the 10,000 MCSs. The results of the direct simulation approach and multiscale simulation approach exhibit very good agreement, indicating good effectiveness of the proposed multiscale approach. Similar analyses on mode shape and MAC values can be also conducted but are not presented here as they are shown to be insensitive to the mesh size effects in the previous section.

To gain a more quantitative insight into the results of probabilistic modal analysis and the mesh size effects, the statistics of the modal frequencies based on meshes with different sizes are summarized in Table 2. For modal frequencies of different orders, the probabilistic modal analysis with different mesh sizes provide almost identical results. There is, however, a slight but notable phenomenon that the higher order modal frequencies (e.g., sixth-order modal frequencies) exhibit a tiny increasing trend with the increasing mesh sizes. The sixth-order modal frequencies increase from 484.78 to 487.42 when the mesh size in modal analysis is enlarged by eight times.

4.3. Parametric Study on COV. Since the COV and correlation at different scales are essentially affected by the COV and correlation at the reference scale (the mean remains constant at different scales), it is then of interest to study the general relations between the COV and correlation at different scales for different values of COV and scales of fluctuation. For such purposes, parametric studies on the COV and the scale of fluctuation were conducted. With the COV of Young's modulus at the reference scale changing from 0 to 0.2, COV and correlation at the coarse scales can be calculated. Figure 11 presents the results of COV and correlation at the coarse scales for different values of COV at the reference scale. Two main observations can be made based on these results. First, the COV at a coarse scale increases linearly with the increasing COV at the reference scale, while the increasing ratio decreases with the increasing mesh sizes. Second, the correlation at a coarse scale is independent from the COV at the reference scale no matter what size of mesh at the coarse scale is used.

Figure 12 shows the evaluation of the statistics of the modal frequency with the increase of the COV at the reference scale. The mean of modal frequencies exhibits a tiny yet notable decreasing profile with the increasing COV at the reference scale. When COV increases from 0.02 to 0.2, the mean of the first modal frequency exhibits a decrease of about 1.1% (i.e., from 13.49 to 13.34). The variation of the COV of modal frequency is more significant than the mean. It increases almost linearly with the increasing COV at the reference scale. The COV of the first-order modal frequency is about 0.05 when the COV of Young's modulus at the reference scale increases to 0.2.

Figure 13 presents the results of MAC values for different values of COV at the reference scale. The MAC values are calculated based on the mode shapes of the heterogeneous case and the homogeneous case. Similar to the evolution profile of modal frequencies, the mean of the MAC values decreases and the COV increases with the increasing COV at the reference scale. When the COV at the reference scale increases to 0.2, the difference between the MAC mean and unity is less than one thousandth, and the MAC COV is also less than 0.001. Overall, the results indicate that material heterogeneity exhibits minimal impacts on mode shapes.

4.4. Parametric Study on Scale of Fluctuation. Lastly, the random field statistics and modal parameters for different scales of fluctuation are analyzed. Figure 14 presents the results of the COV and correlation with the scale of fluctuation increasing from 10 to 50 m. With an increase in the scale of fluctuation, the COV at the target scale increases and approaches the COV at the reference scale; the correlation decreases and approaches the correlation calculated at the reference scale. Generally, a random field would exhibit severe variations in space if the scale of fluctuation is small, and it would appear as a homogeneous field if the scale of fluctuation approaches infinite. In the case of a homogeneous field, the material property is the same everywhere in the domain and becomes a single random variable. The results indicate that the effects of mesh size on the random field statistics become less significant with the increase of scale of fluctuation.

The statistics of the first-order modal frequency for different scales of fluctuation are presented in Figure 15. Although the mean of the modal frequency exhibits an increasing trend with the increasing scale of fluctuation, the variation of the mean is deemed to be negligible, i.e., less than 0.1%. The COV of the modal frequency increases as the scale of fluctuation increases. This is reasonable because the COV increases and the correlation of the random fields decreases with the increase in the scale of fluctuation. The increase of COV and decrease of correlation indicates a greater variation in the material property fields and thus results in a greater variation in the modal parameters. The COV of the modal frequency exhibits considerably significant variations (i.e., increases from about 0.016 to 0.028), when the scale of fluctuation changes from 10 to 50 m.

The statistics of the first-order MAC values for different scales of fluctuation are presented in Figure 16. Although the mean of the MAC values first decreases and then increases while the COV first increases and then decreases with the increasing scale of fluctuation, the variations in the mean and COV are next to negligible. Based on the results of probabilistic modal analysis with different mesh sizes and different random field statistics, it is indicated that material heterogeneity has considerably significant impacts on modal frequencies and should be considered in applications such as reliability-based structural damage identification, while it has negligible impacts on mode shapes as well as MAC values and thus could be ignored in such applications for computational simplicity.

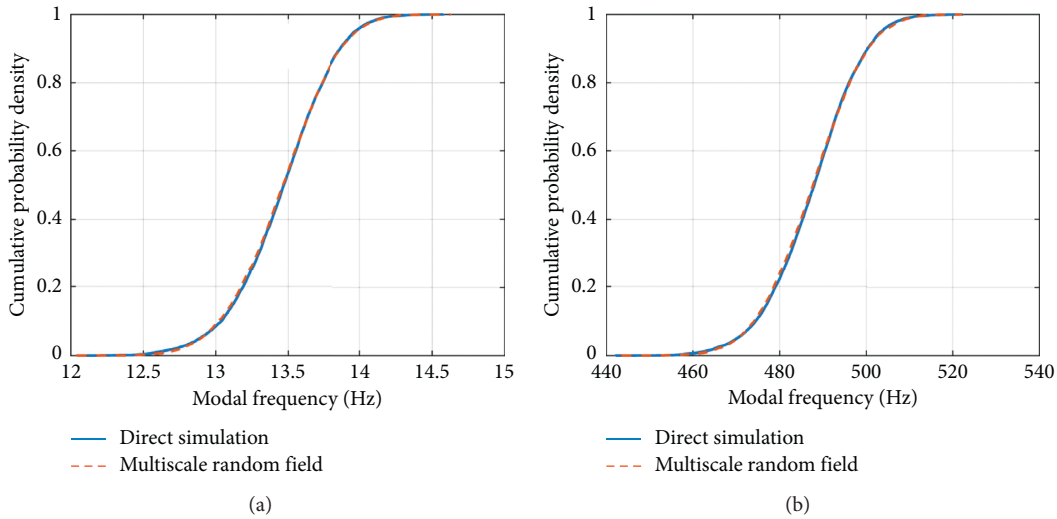

Figure 10: The cumulative distribution of modal frequencies based on the 10,000 MCSs: (a) first-order modal frequency and (b) sixth-order modal frequency.

Table 2: Modal frequencies based on the meshes with different sizes.

Mesh size (m)	Modal frequency (mean ± standard deviation, Hz)					
	1st	2nd	3rd	4th	5th	6th
0.5	13.45 ± 0.33	53.84 ± 1.19	121.17 ± 2.61	215.42 ± 4.58	336.64 ± 7.11	484.78 ± 10.20
1.0	13.46 ± 0.33	53.86 ± 1.19	121.21 ± 2.59	215.52 ± 4.55	336.78 ± 7.06	485.02 ± 10.15
1.5	13.45 ± 0.33	53.85 ± 1.19	121.20 ± 2.60	215.50 ± 4.56	336.80 ± 7.07	485.07 ± 10.16
2.0	13.45 ± 0.33	53.86 ± 1.19	121.23 ± 2.59	215.59 ± 4.53	336.97 ± 7.04	485.42 ± 10.12
2.5	13.46 ± 0.33	53.88 ± 1.19	121.30 ± 2.59	215.72 ± 4.55	337.23 ± 7.09	485.90 ± 10.17
3.0	13.46 ± 0.33	53.87 ± 1.18	121.29 ± 2.57	215.76 ± 4.53	337.37 ± 7.05	486.26 ± 10.12
4.0	13.45 ± 0.33	53.87 ± 1.20	121.31 ± 2.62	215.88 ± 4.60	337.81 ± 7.17	487.42 ± 10.31

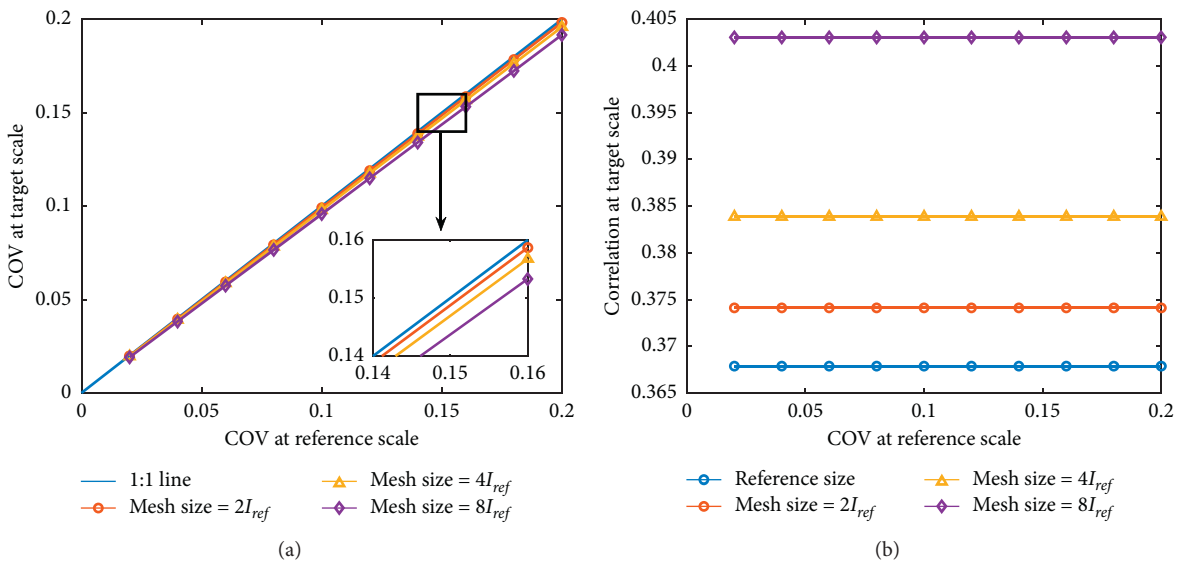

Figure 11: Random field statistics for different values of COV at the reference scale: (a) COV at the target scale and (b) correlation at the target scale when the separation distance is 16 m (i.e., about half of the scale of fluctuation).

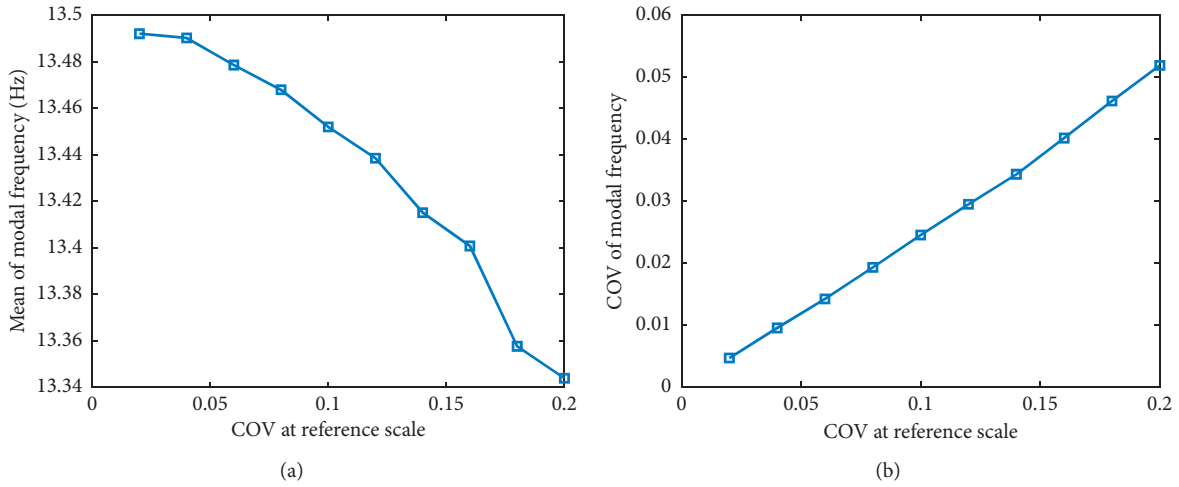

Figure 12: Statistics of the first-order modal frequency for different values of COV at the reference scale: (a) mean and (b) COV. The mesh size is 4 times the reference size.

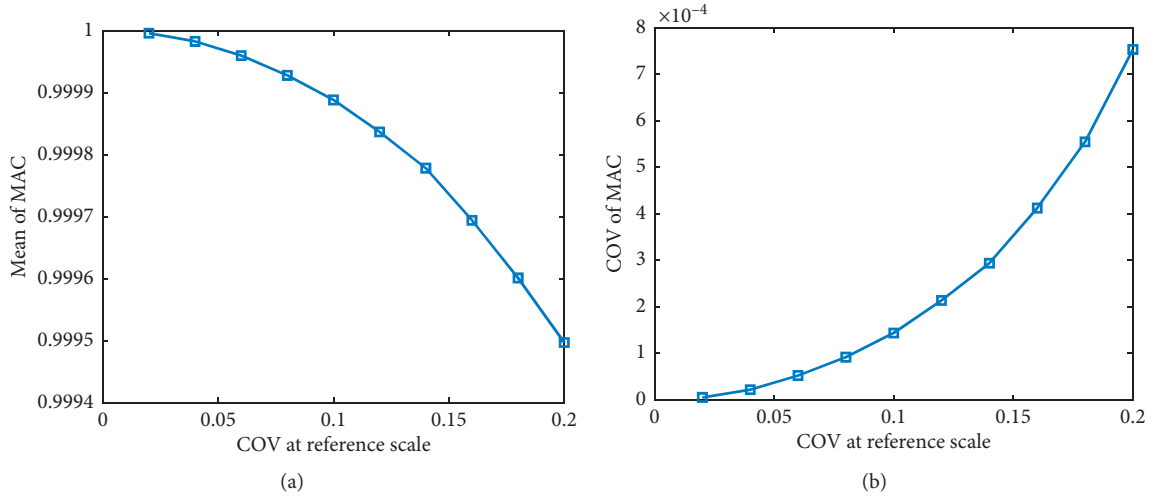

Figure 13: Statistics of the first-order MAC values for different values of COV at the reference scale: (a) mean and (b) COV. The mesh size is 4 times the reference size.

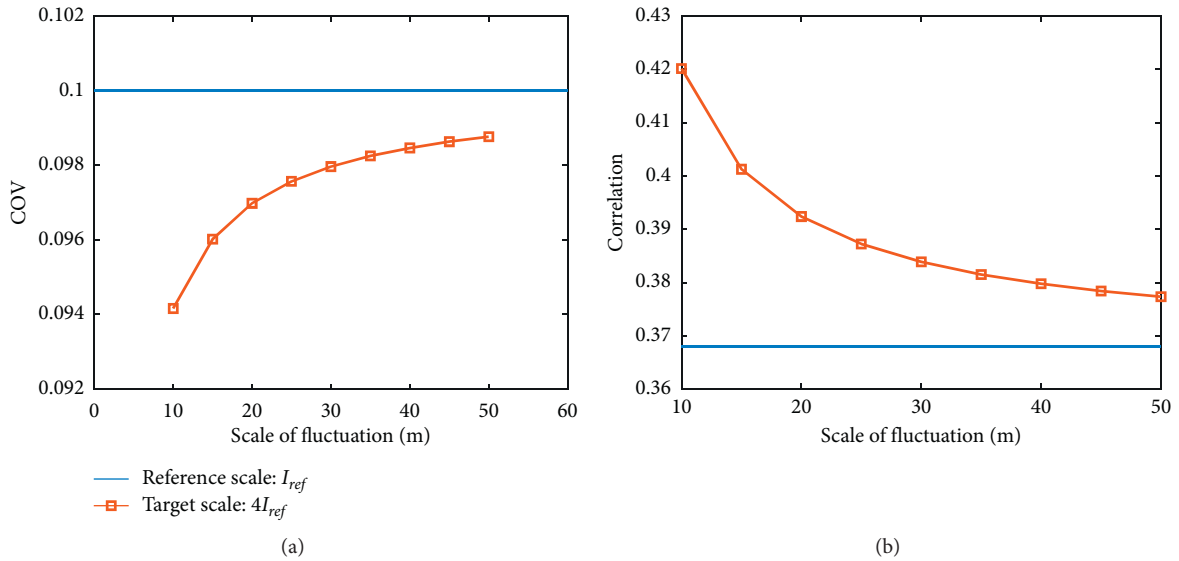

Figure 14: Random field statistics at the target scale for different scales of fluctuation: (a) COV and (b) correlation when the separation distance is half of the scale of fluctuation.

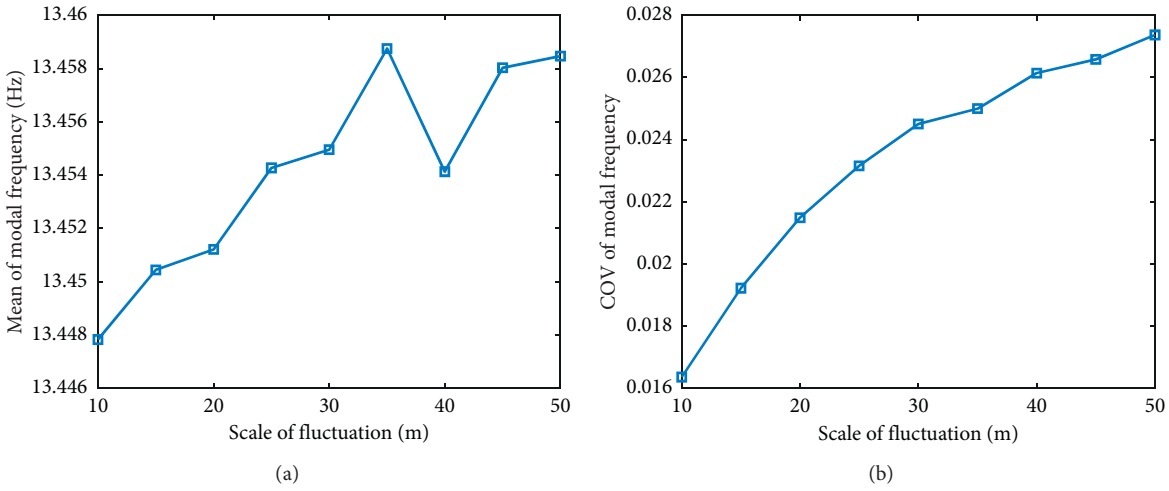

Figure 15: Statistics of the first-order modal frequency for different scales of fluctuation: (a) mean and (b) COV. The mesh size is 4 times the reference size.

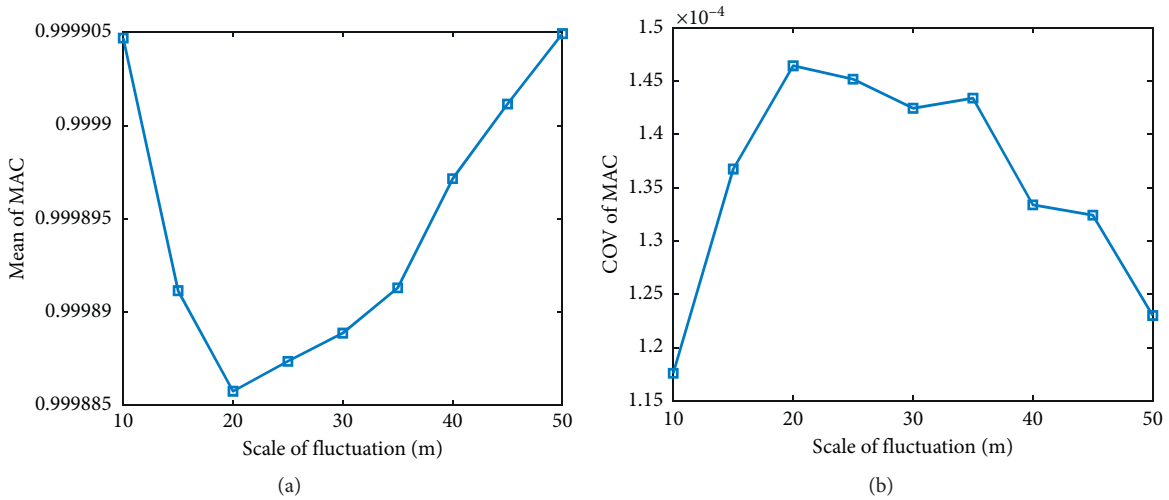

Figure 16: Statistics of the first-order MAC values for different scales of fluctuation: (a) mean and (b) COV. The mesh size is 4 times the reference size.

5. Conclusions

The statistics (e.g., mean, variance, and scale of fluctuation) of a material property would have different values at different length scales due to the spatially averaging effects. This work presents a framework for the probabilistic modal analysis of beam structures with random field models at multiple scales. An approach of evaluating random field parameters and generating random field material properties at different scales is developed based on element averaging. Probabilistic analysis of a simply supported beam is performed as an example, and the validity of the multiscale random field approach and the effects of random field properties on structure modal parameters are investigated. With the results presented, the following conclusions can be drawn.

(1) The uncertainty in a material property decreases, whereas the correlation increases with the increase of element size due to the spatially averaging effects, while the mean remains constant. Heterogeneous material properties with different element sizes can be effectively generated using the developed multiscale random field approach.

(2) There is relatively significant uncertainty in the modal frequencies as a result of the heterogeneous material properties, while the uncertainty in mode shapes is considerably small. The structural dynamics can be accurately characterized using the multiscale random field approach, which allows for the usage of coarse meshes in the FE simulations and thus improves the computational efficiency.

(3) The uncertainty in a material property characterized at a coarser scale increases with the uncertainty at the reference scale, while the correlation remains unchangeable with respect to the variation of uncertainty at the reference scale. With an increase in the

scale of fluctuation at the reference scale, the uncertainty at a coarser scale increases, whereas the correlation at a coarser scale decreases.

(4) The uncertainty in modal frequencies increases with the uncertainty in material properties, and it also increases with the increase of the scale of fluctuation. Material heterogeneity has considerably significant impacts on modal parameters and should be properly considered in applications such as structure reliability analysis.

Data Availability

The data used to support the findings of this study are available from the corresponding author upon request.

Conflicts of Interest

The author declares that there are no conflicts of interest.

Acknowledgments

This study was supported by the National Foundation of China under grant no. 51108472. The support is gratefully acknowledged. The author would like to appreciate the comments and discussions from Prof. Junjun Zheng at Economics and Management School of Wuhan University.

References

[1] J. E. Padgett and C. Tapia, "Sustainability of natural hazard risk mitigation: life cycle analysis of environmental indicators for bridge infrastructure," *Journal of Infrastructure Systems*, vol. 19, no. 4, pp. 395–408, 2013.

[2] R. Sebastian, "Asset management business model for design, realization, and maintenance of fibre reinforced polymer bridges," *Advances in Civil Engineering*, vol. 1, 2013.

[3] J.-S. Tan, K. Elbaz, Z.-F. Wang, J. S. Shen, and J. Chen, "Lessons learnt from bridge collapse: a view of sustainable management," *Sustainability*, vol. 12, no. 3, p. 1205, 2020.

[4] Z. Fu and J. He, *Modal Analysis*, Elsevier, Amsterdam, Netherlands, 2001.

[5] L. Wang, M. Huang, and Z.-R. Lu, "Blind separation of structural modes by compact-bandwidth regularization," *Mechanical Systems and Signal Processing*, vol. 131, pp. 288–316, 2019.

[6] B. Ellingwood and A. Tallin, "Structural serviceability: floor vibrations," *Journal of Structural Engineering*, vol. 110, no. 2, pp. 401–418, 1984.

[7] R. Alkhatib and M. F. Golnaraghi, "Active structural vibration control: a review," *The Shock and Vibration Digest*, vol. 35, no. 5, p. 367, 2003.

[8] C. Cui, R. Ma, X. Hu, and W. He, "Vibration analysis for pendent pedestrian path of a long-span extradosed bridge," *Sustainability*, vol. 11, no. 17, p. 4664, 2019.

[9] J.-s. Hwang, A. Kareem, and W.-j. Kim, "Estimation of modal loads using structural response," *Journal of Sound and Vibration*, vol. 326, no. 3-5, pp. 522–539, 2009.

[10] A. Tatar, A. Niousha, and F. R. Rofooei, "Damage detection in existing reinforced concrete building using forced vibration test based on mode shape data," *Journal of Civil Structural Health Monitoring*, vol. 7, no. 1, pp. 123–135, 2017.

[11] M. Alwash, B. F. Sparling, and L. D. Wegner, "Influence of excitation on dynamic system identification for a multi-span reinforced concrete bridge," *Advances in Civil Engineering*, vol. 1, 2009.

[12] E. P. Carden and P. Fanning, "Vibration based condition monitoring: a review," *Structural Health Monitoring: An International Journal*, vol. 3, no. 4, pp. 355–377, 2004.

[13] Y. Zhang, C.-W. Kim, and J. Lin, "Removing environmental influences in health monitoring for steel bridges through copula approaches," *International Journal of Steel Structures*, vol. 19, no. 3, pp. 888–895, 2019.

[14] J. K. Sinha, M. I. Friswell, and S. Edwards, "Simplified models for the location of cracks in beam structures using measured vibration data," *Journal of Sound and Vibration*, vol. 251, no. 1, pp. 13–38, 2002.

[15] G. Chellini, G. De Roeck, L. Nardini, and W. Salvatore, "Damage analysis of a steel-concrete composite frame by finite element model updating," *Journal of Constructional Steel Research*, vol. 66, no. 3, pp. 398–411, 2010.

[16] A. C. Altunı¸sık, F. Y. Okur, and V. Kahya, "Structural identification of a cantilever beam with multiple cracks: modeling and validation," *International Journal of Mechanical Sciences*, vol. 130, pp. 74–89, 2017.

[17] Y.-L. Xu, C.-D. Zhang, S. Zhan, and B. F. Spencer, "Multi-level damage identification of a bridge structure: a combined numerical and experimental investigation," *Engineering Structures*, vol. 156, pp. 53–67, 2018.

[18] M. B. Jaksa, J. S. Goldsworthy, G. A. Fenton et al., "Towards reliable and effective site investigations," *Géotechnique*, vol. 55, no. 2, pp. 109–121, 2005.

[19] T. Elkateb, R. Chalaturnyk, and P. K. Robertson, "An overview of soil heterogeneity: quantification and implications on geotechnical field problems," *Canadian Geotechnical Journal*, vol. 40, no. 1, pp. 1–15, 2003.

[20] Q. Chen, A. Seifried, J. E. Andrade, and J. W. Baker, "Characterization of random fields and their impact on the mechanics of geosystems at multiple scales," *International Journal for Numerical and Analytical Methods in Geomechanics*, vol. 36, no. 2, pp. 140–165, 2012.

[21] H. Zhu and L. M. Zhang, "Characterizing geotechnical anisotropic spatial variations using random field theory," *Canadian Geotechnical Journal*, vol. 50, no. 7, pp. 723–734, 2013.

[22] W. Liu, Q. Chen, C. Wang, C. H. Juang, and G. Chen, "Spatially correlated multiscale V s30 mapping and a case study of the Suzhou site," *Engineering Geology*, vol. 220, pp. 110–122, 2017.

[23] M. K. Lo and Y. F. Leung, "Probabilistic analyses of slopes and footings with spatially variable soils considering cross-correlation and conditioned random field," *Journal of Geotechnical and Geoenvironmental Engineering*, vol. 143, Article ID 04017044, 2017.

[24] Y. Liu, Y. Pan, M. Sun, J. Hu, and K. Yao, "Lateral compression response of overlapping jet-grout columns with geometric imperfections in radius and position," *Canadian Geotechnical Journal*, vol. 55, no. 9, pp. 1282–1294, 2018.

[25] Q. Huang, P. Gardoni, and S. Hurlebaus, "A probabilistic damage detection approach using vibration-based nondestructive testing," *Structural Safety*, vol. 38, pp. 11–21, 2012.

[26] C. Su, W. Liao, L. Tan, and R. Chen, "Reliability-based damage identification using dynamic signatures," *Journal of Bridge Engineering*, vol. 21, Article ID 04015058, 2016.

[27] J. J. Moughty and J. R. Casas, "A state of the art review of modal-based damage detection in bridges: development,

challenges, and solutions," *Applied Sciences*, vol. 7, no. 5, p. 510, 2017.

[28] S.-E. Fang, S. Chen, Y.-Q. Lin, and Z.-L. Dong, "Probabilistic damage identification incorporating approximate Bayesian computation with stochastic response surface," *Mechanical Systems and Signal Processing*, vol. 128, pp. 229–243, 2019.

[29] Z. Ding, J. Li, H. Hao, and Z.-R. Lu, "Structural damage identification with uncertain modelling error and measurement noise by clustering based tree seeds algorithm," *Engineering Structures*, vol. 185, pp. 301–314, 2019.

[30] M. DeGroot and M. Schervish, *Probability and Statistics*, Pearson Education, London, UK, 2012.

[31] D.-Q. Li, S.-H. Jiang, Z.-J. Cao, W. Zhou, C.-B. Zhou, and L.-M. Zhang, "A multiple response-surface method for slope reliability analysis considering spatial variability of soil properties," *Engineering Geology*, vol. 187, pp. 60–72, 2015.

[32] Y. Wang, Z. Cao, and D. Li, "Bayesian perspective on geotechnical variability and site characterization," *Engineering Geology*, vol. 203, pp. 117–125, 2016.

[33] W. Gong, Y.-M. Tien, C. H. Juang, J. R. Martin, and Z. Luo, "Optimization of site investigation program for improved statistical characterization of geotechnical property based on random field theory," *Bulletin of Engineering Geology and the Environment*, vol. 76, no. 3, pp. 1021–1035, 2017.

[34] L. Huang, S. Huang, and Z. Lai, "On the optimization of site investigation programs using centroidal Voronoi tessellation and random field theory," *Computers and Geotechnics*, vol. 118, Article ID 103331, 2020.

[35] R. Baker, "Modeling soil variability as a random field," *Journal of the International Association for Mathematical Geology*, vol. 16, no. 5, pp. 435–448, 1984.

[36] K.-K. Phoon and F. H. Kulhawy, "Evaluation of geotechnical property variability," *Canadian Geotechnical Journal*, vol. 36, no. 4, pp. 625–639, 1999.

[37] D. V. Griffiths and G. A. Fenton, "Bearing capacity of spatially random soil: the undrained clay Prandtl problem revisited," *Géotechnique*, vol. 51, no. 4, pp. 351–359, 2001.

[38] Y. Pan, Y. Liu, A. Tyagi, F.-H. Lee, and D.-Q. Li, "Model-independent strength-reduction factor for effect of spatial variability on tunnel with improved soil surrounds," *Géotechnique*, vol. 71, pp. 1–17, 2020.

[39] Y. Pan, Y. Liu, F. H. Lee, and K. K. Phoon, "Analysis of cement-treated soil slab for deep excavation support - a rational approach," *Géotechnique*, vol. 69, no. 10, pp. 888–905, 2019.

[40] D. V. Griffiths, J. Huang, and G. A. Fenton, "Probabilistic infinite slope analysis," *Computers and Geotechnics*, vol. 38, no. 4, pp. 577–584, 2011.

[41] D. V. Griffiths, G. A. Fenton, and N. Manoharan, "Bearing capacity of rough rigid strip footing on cohesive soil: probabilistic study," *Journal of Geotechnical and Geoenvironmental Engineering*, vol. 128, no. 9, pp. 743–755, 2002.

[42] Z. Lai, Q. Chen, C. Wang, and X. Zhou, "Modeling dynamic responses of heterogeneous seabed with embedded pipeline through multiresolution random field and coupled hydro-mechanical simulations," *Ocean Engineering*, vol. 173, pp. 556–570, 2019.

[43] L. L. Zhang, Y. Cheng, J. H. Li, X. L. Zhou, D. S. Jeng, and X. Y. Peng, "Wave-induced oscillatory response in a randomly heterogeneous porous seabed," *Ocean Engineering*, vol. 111, pp. 116–127, 2016.

[44] M. Shen, C. H. Juang, and Q. Chen, "Mitigation of liquefaction hazard by dynamic compaction - a random field perspective," *Canadian Geotechnical Journal*, vol. 56, no. 12, pp. 1803–1815, 2019.

[45] Y. F. Leung, W. Liu, J.-S. Li et al., "Three-dimensional spatial variability of arsenic-containing soil from geogenic source in Hong Kong: implications on sampling strategies," *Science of the Total Environment*, vol. 633, pp. 836–847, 2018.

[46] X. Y. Peng, L. L. Zhang, D. S. Jeng, L. H. Chen, C. C. Liao, and H. Q. Yang, "Effects of cross-correlated multiple spatially random soil properties on wave-induced oscillatory seabed response," *Applied Ocean Research*, vol. 62, pp. 57–69, 2017.

[47] L. Li and X. Chu, "Failure mechanism and factor of safety for spatially variable undrained soil slope," *Advances in Civil Engineering*, vol. 1, 2019.

[48] W. Gong, C. H. Juang, J. R. Martin, H. Tang, Q. Wang, and H. Huang, "Probabilistic analysis of tunnel longitudinal performance based upon conditional random field simulation of soil properties," *Tunnelling and Underground Space Technology*, vol. 73, no. 73, pp. 1–14, 2018.

[49] L. Huang, S. Huang, and Z. Lai, "On an energy-based criterion for defining slope failure considering spatially varying soil properties," *Engineering Geology*, vol. 264, Article ID 105323, 2020.

[50] M. A. Hicks and C. Onisiphorou, "Stochastic evaluation of static liquefaction in a predominantly dilative sand fill," *Géotechnique*, vol. 55, no. 2, pp. 123–133, 2005.

[51] R. Jamshidi Chenari and H. Kamyab Farahbakhsh, "Generating non-stationary random fields of auto-correlated, normally distributed CPT profile by matrix decomposition method," *Georisk: Assessment and Management of Risk for Engineered Systems and Geohazards*, vol. 9, no. 2, pp. 96–108, 2015.

[52] X. Li, L. Zhang, and J. Li, "Using conditioned random field to characterize the variability of geologic profiles," *Journal of Geotechnical and Geoenvironmental Engineering*, vol. 142, Article ID 04015096, 2015.

[53] O. Perrin and R. Senoussi, "Reducing non-stationary random fields to stationarity and isotropy using a space deformation," *Statistics & Probability Letters*, vol. 48, no. 1, pp. 23–32, 2000.

[54] M. Davis, "Production of conditional simulations via the LU triangular decomposition of the covariance matrix," *Mathematical Geology*, vol. 19, pp. 91–98, 1987.

[55] S. E. Cho and H. C. Park, "Effect of spatial variability of cross-correlated soil properties on bearing capacity of strip footing," *International Journal for Numerical and Analytical Methods in Geomechanics*, vol. 34, no. 1, pp. 1–26, 2010.

[56] Z.-P. Deng, D.-Q. Li, X.-H. Qi, Z.-J. Cao, and K.-K. Phoon, "Reliability evaluation of slope considering geological uncertainty and inherent variability of soil parameters," *Computers and Geotechnics*, vol. 92, pp. 121–131, 2017.

[57] B. Sudret and A. Der Kiureghian, *Stochastic Finite Element Methods and Reliability: A State-Of-The-Art Report*, Department of Civil and Environmental Engineering, University of California, Berkeley, California, 2000.

[58] A. Der Kiureghian and J.-B. Ke, "The stochastic finite element method in structural reliability," *Probabilistic Engineering Mechanics*, vol. 3, no. 2, pp. 83–91, 1988.

[59] S.-H. Jiang, D.-Q. Li, L.-M. Zhang, and C.-B. Zhou, "Slope reliability analysis considering spatially variable shear strength parameters using a non-intrusive stochastic finite element method," *Engineering Geology*, vol. 168, pp. 120–128, 2014.

[60] L.-L. Liu, Y.-M. Cheng, Q.-J. Pan, and D. Dias, "Incorporating stratigraphic boundary uncertainty into reliability analysis of slopes in spatially variable soils using one-dimensional

conditional Markov chain model," *Computers and Geotechnics*, vol. 118, Article ID 103321, 2020.

[61] S.-H. Jiang, J. Huang, and C.-B. Zhou, "Efficient system reliability analysis of rock slopes based on subset simulation," *Computers and Geotechnics*, vol. 82, pp. 31–42, 2017.

[62] Q. Pan and D. Dias, "An efficient reliability method combining adaptive support vector machine and Monte Carlo simulation," *Structural Safety*, vol. 67, pp. 85–95, 2017.

[63] Q. Pan, X. Qu, L. Liu, and D. Dias, "A sequential sparse polynomial chaos expansion using Bayesian regression for geotechnical reliability estimations," *International Journal for Numerical and Analytical Methods in Geomechanics*, vol. 44, no. 6, pp. 874–889, 2020.

[64] M. Pastor, M. Binda, and T. Harčarik, "Modal assurance criterion," *Procedia Engineering*, vol. 48, pp. 543–548, 2012.